Spin echo

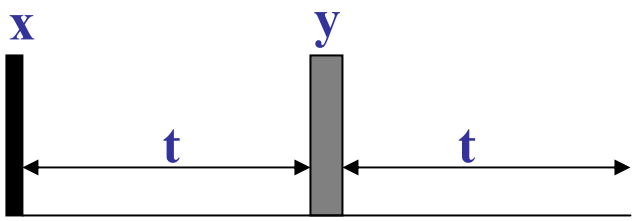

$\frac{1}{2}\pi I_x - t - \pi I_y - t$

t : as needed, not correlated with 1/J.

Functions: 1. refocusing; 2. decoupling.

- Chemical shift evolution is refocused by the spin-echo.
- Heteronuclear J-couplings evolution are refocused by a spin-echo. Because only one spin experiences a 180° pulse.
- Homonuclear couplings evolution are not refocused by a spin-echo. Because both spins experiences a 180° pulse.

- It's also used for decoupling H^1-N^{15} by refocusing the H^1 magnetization.

Hahn echo

In 1950, Erwin Hahn first detected echoes in NMR, he applied two successive 90° pulses separated by a short delay time. This was further developed by Carr and Purcell who used a 180° refocusing pulse to replace the second pulse. Spin echoes are sometimes also called Hahn echoes.

Hahn, E.L. (1950). "Spin echoes". Physical Review. 80: 580–594.
Carr, H. Y.; Purcell, E. M. (1954). "Effects of Diffusion on Free Precession in Nuclear Magnetic Resonance Experiments". Physical Review. 94: 630–638.

Advantages:

1. **Baseline distortions can be removed. (it's originally introduced by Rance and Byrd.)**
2. **Water suppression was significantly improved due to the refocusing properties of the 180° pulse, which reduces the effect of inhomogeneous broadening at the base of the residual water peak.**

2D NOESY

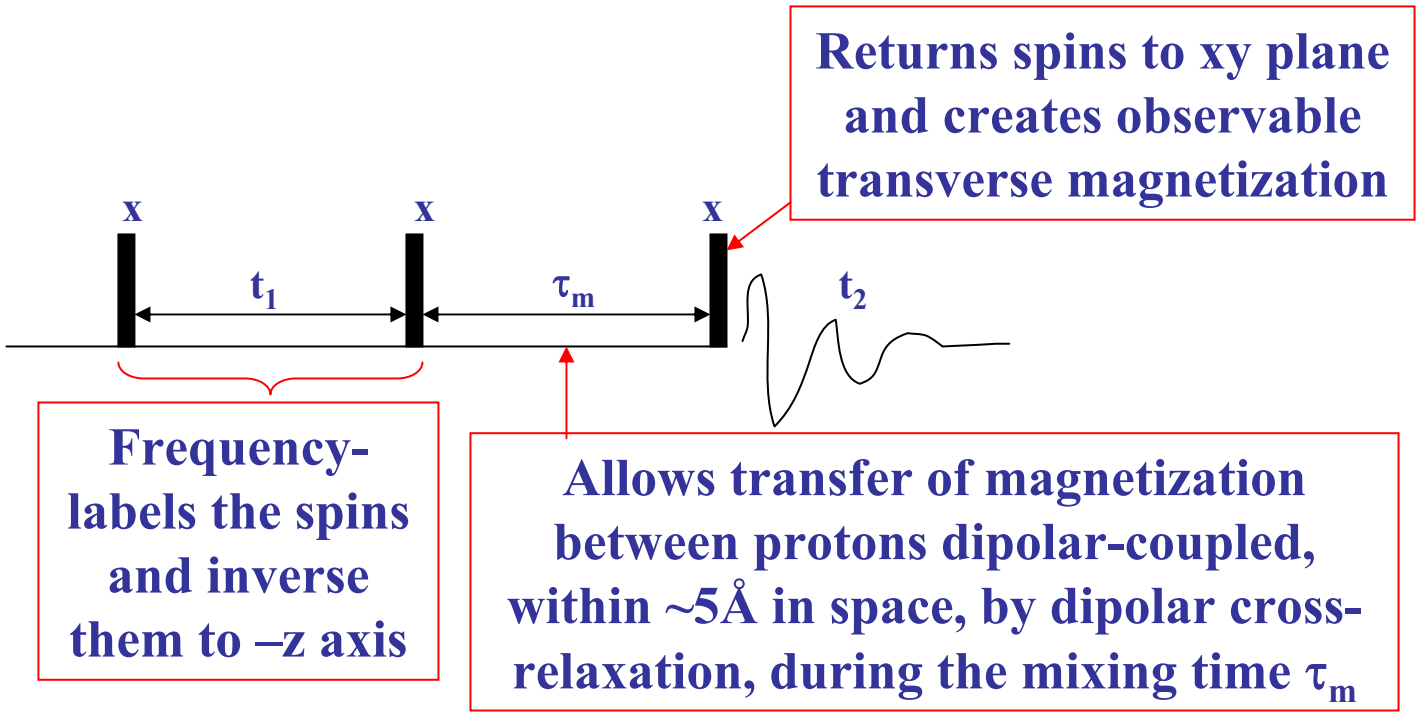

After the final $(90°)_x$, a Hahn echo sequence $(-\Delta_1 - \pi I_y - \Delta_2)$ can be added for improvement of flatness of baseline.

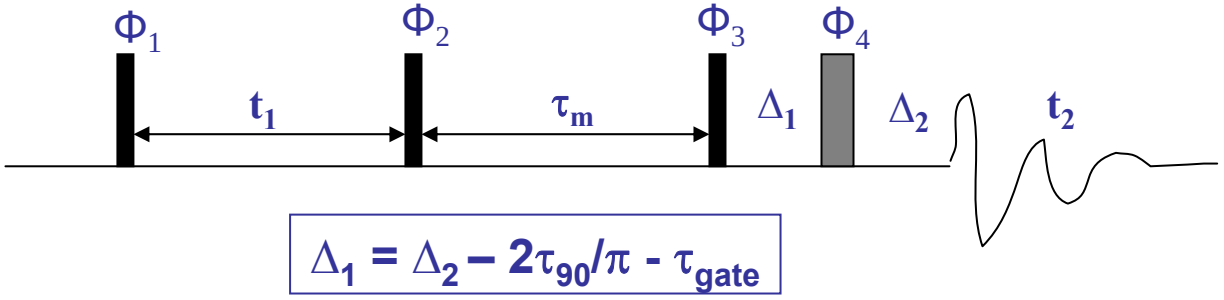

$$\Delta_1 = \Delta_2 - 2\tau_{90}/\pi - \tau_{gate}$$

JR-NOESY: NOESY with a jump-return observe pulse

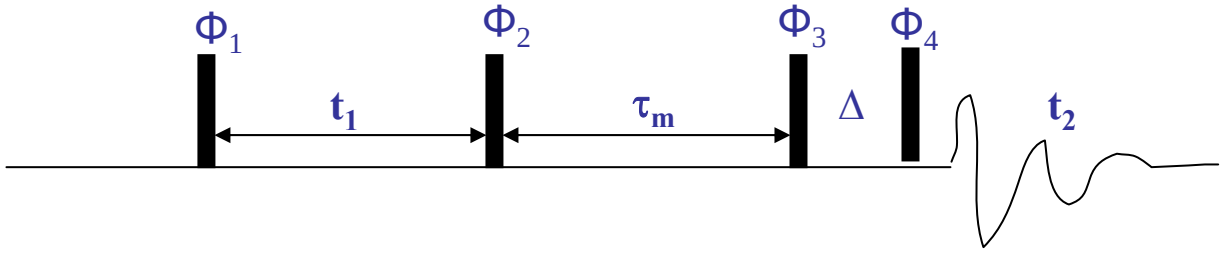

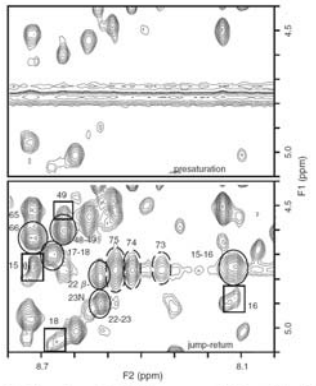

FIGURE 6.55 Comparison of NOESY spectra acquired from H_2O solution in which solvent was suppressed by presaturation (top) or selective excitation with a jump–return sequence (bottom). The spectra were collected under identical conditions except for the mixing times, which were 100 and 150 ms in presaturation and jump–return spectra, respectively. Intraresidue and sequential NOEs are denoted by rectangles and ellipses, respectively, with the peaks arising between $^1H^N$ and $^1H^\alpha$ unless otherwise noted. The three peaks outlined by broken ellipses probably arise from exchange of amide protons with the solvent, as residues 73 to 75 are close to the C-terminus and are flexible.

- Much more peaks near the water peak can be shown up than presat method.
- Δ delay (~100us) and the length of the last pulse need to be optimized.

Relayed NOESY

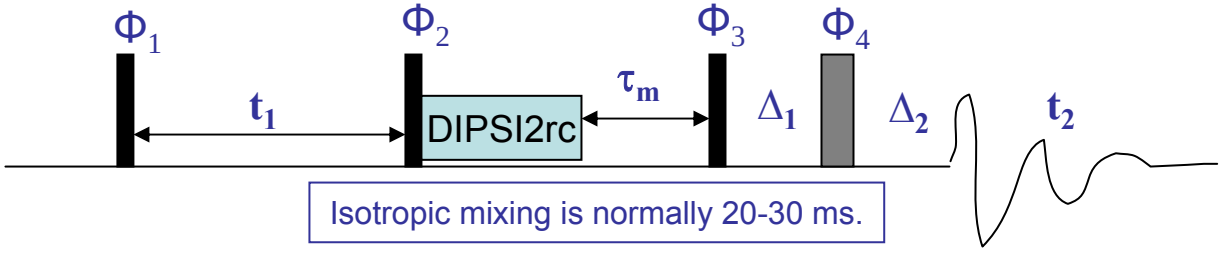

Isotropic mixing is normally 20-30 ms.

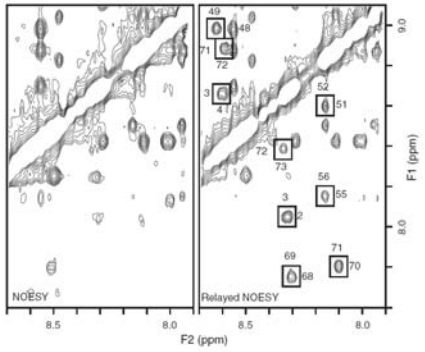

FIGURE 6.58 Comparison of sections of NOESY (left) and relayed NOESY (right) spectra. Both experiments were performed under identical conditions except for the mixing period, which included 27 ms of DIPSI-2rc isotropic mixing in the relayed NOESY. Weak coherent irradiation was used to suppress the solvent before the experiment and during the 100-ms NOE mixing period. Relayed NOESY peaks outlined by boxes indicate sequential $^1H^N$–$^1H^N$ NOEs between residues in the β-sheet of ubiquitin that are weak or not observed in the conventional NOESY experiment. The greater intensity allows sequential assignments to be made even if sequential $^1H^\alpha$ resonances are degenerate (as is the case for His68 and Leu69). The labels denote residue numbers of the amide protons contributing to each cross-peak.

For sequential assignment purpose, not for NOE distance information.

INEPT – Insensitive Nucleus Enhanced by Polarization Transfer

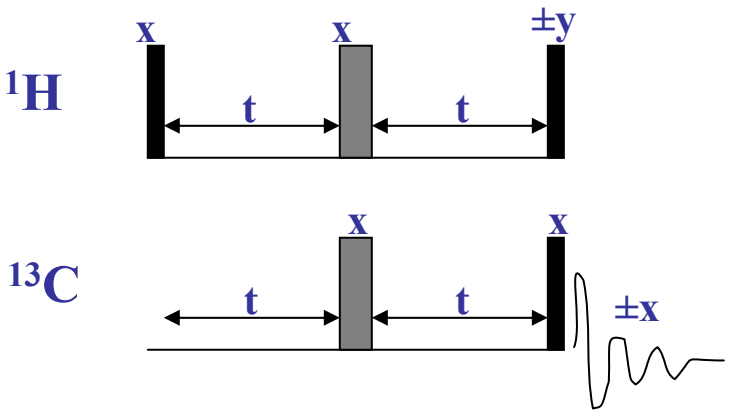

$t = 1/(4*{}^1J_{CH}) = 1/(4*212Hz) = 1.18ms$

INEPT sequence: transfer of population differences from ^{1}H to X (X: ^{13}C, ^{15}N etc. ^{1}H and X are J-coupling interaction), (by inversion of populations of proton, → changing populations of spin X). It can enhance signal intensity of X by γ_H/γ_X (^{13}C, ~4; ^{15}N, ~10) , and is widely used in NMR experiments.

Refocused INEPT and Product operator analysis: — right hand rule

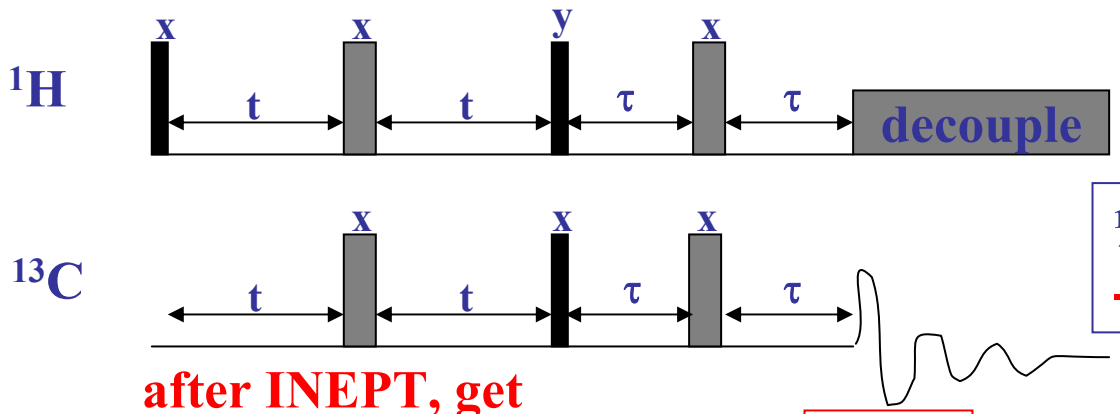

$\frac{1}{2}\pi I_x$ - t - $\pi(I_x+S_x)$ - t - $\frac{1}{2}\pi(I_y+S_x)$ - τ - $\pi(I_x+S_x)$ - τ

after INEPT, get anti-phase component

$-2I_zS_y$

$2I_zS_z$

τ

$-2I_zS_y\cos(\pi J\tau)$

πI_x

$+2I_zS_y\cos(\pi J\tau)$

πS_x

$-2I_zS_y\cos(\pi J\tau)$

τ

$-2I_zS_y\cos(\pi J\tau)\bullet\cos(\pi J\tau)$

$-2I_zS_y$

If $\tau = 1/(4J)$,

τ

$+S_x\cos(\pi J\tau)\bullet\sin(\pi J\tau)$

$+S_x$

In-phase component

τ

$+S_x\sin(\pi J\tau)$

πI_x

$+S_x\sin(\pi J\tau)$

πS_x

$+S_x\sin(\pi J\tau)$

τ

$+S_x\sin(\pi J\tau)\bullet\cos(\pi J\tau)$

τ

$+2I_zS_y\sin(\pi J\tau)\bullet\sin(\pi J\tau)$

$+2I_zS_y$

Reverse INEPT --- the reverse transfer is achieved.

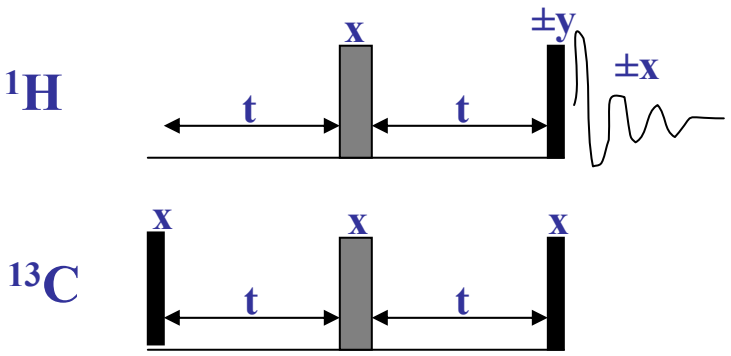

$t = 1/(4*{}^1J_{CH}) = 1/(4*212Hz) = 1.18ms$

In real 2D or 3D expt., the first 90 pulse on the ^{13}C is not needed because the antiphase magnetization is already present after t1 evolution, the reverse INEPT looks like the following in HSQC:

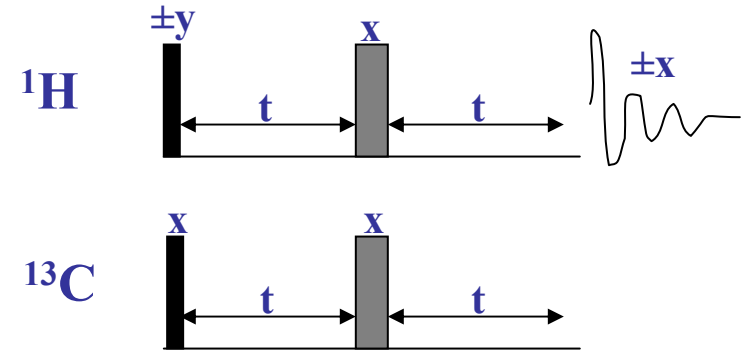

HSQC — Heteronuclear Single-Quantum Coherence

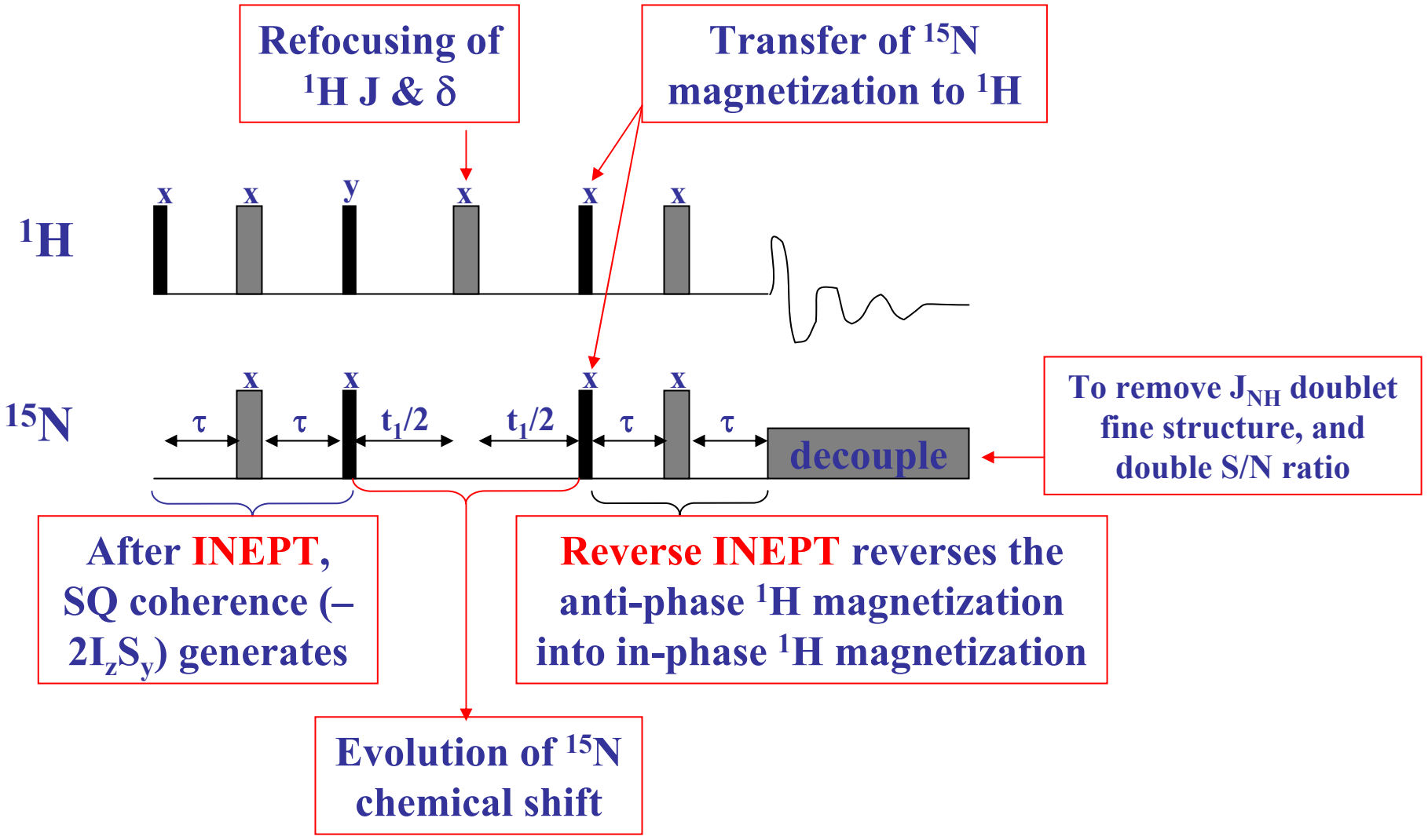

HSQC product operator analysis:

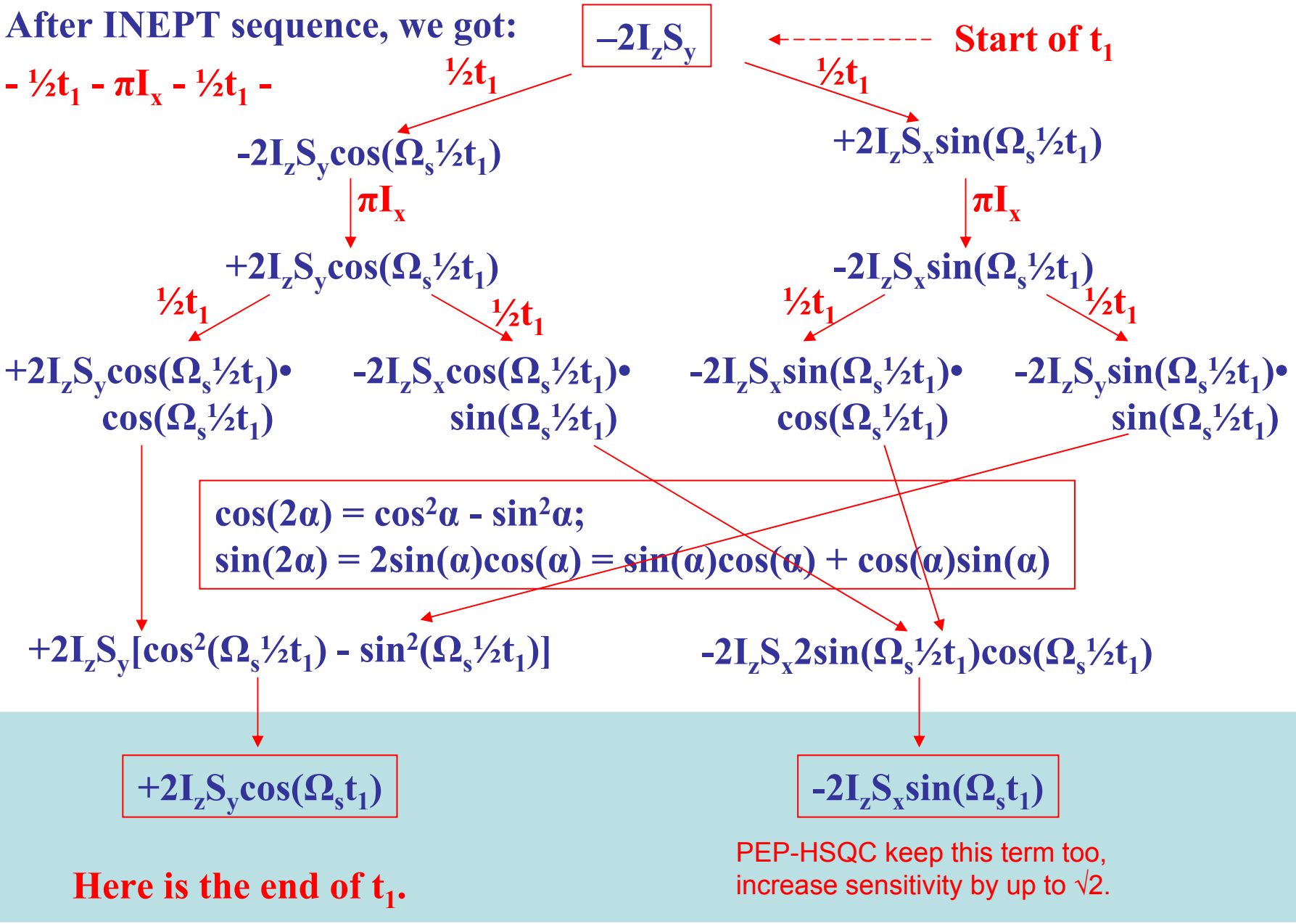

$\frac{1}{2}\pi(I_x + S_x) - \tau - \pi(I_x + S_x) - \tau$

$+2I_zS_y\cos(\Omega_s t_1)$

$\downarrow \frac{1}{2}\pi I_x$

$-2I_yS_y\cos(\Omega_s t_1)$

$\downarrow \frac{1}{2}\pi S_x$

$-2I_yS_z\cos(\Omega_s t_1)$

τ → $-2I_yS_z\cos(\Omega_s t_1)\bullet\cos(\pi J\tau)$

$\downarrow \pi I_x$

$+2I_yS_z\cos(\Omega_s t_1)\bullet\cos(\pi J\tau)$

$\downarrow \pi S_x$

$-2I_yS_z\cos(\Omega_s t_1)\bullet\cos(\pi J\tau)$

τ → $-2I_yS_z\cos(\Omega_s t_1)\bullet\cos(\pi J\tau)\bullet\cos(\pi J\tau)$

If $\tau = 1/(4J)$, → $-I_yS_z\cos(\Omega_s t_1)$

τ → $+I_x\cos(\Omega_s t_1)\bullet\cos(\pi J\tau)\bullet\sin(\pi J\tau)$

τ → $+I_x\cos(\Omega_s t_1)\bullet\sin(\pi J\tau)$

$\downarrow \pi I_x$

$+I_x\cos(\Omega_s t_1)\bullet\sin(\pi J\tau)$

$\downarrow \pi S_x$

$+I_x\cos(\Omega_s t_1)\bullet\sin(\pi J\tau)$

τ → $+I_x\cos(\Omega_s t_1)\bullet\cos(\pi J\tau)\bullet\sin(\pi J\tau)$

τ → $+2I_yS_z\cos(\Omega_s t_1)\bullet\sin(\pi J\tau)\bullet\sin(\pi J\tau)$

$\downarrow$

$+I_yS_z\cos(\Omega_s t_1)$

$-2I_zS_x\sin(\Omega_s t_1)$

$\downarrow \frac{1}{2}\pi I_x$

$+2I_yS_x\sin(\Omega_s t_1)$

$\downarrow \frac{1}{2}\pi S_x$

$+2I_yS_x\sin(\Omega_s t_1)$

τ → $E/2$

τ → $+2I_yS_x\sin(\Omega_s t_1)\bullet\cos(\pi J\tau)$

$\downarrow \pi I_x$

$-2I_yS_x\sin(\Omega_s t_1)\bullet\cos(\pi J\tau)$

πS_x → $-2I_yS_x\sin(\Omega_s t_1)\bullet\cos(\pi J\tau)$

τ → $-2I_yS_x\sin(\Omega_s t_1)\bullet\cos(\pi J\tau)$

$+I_x\cos(\Omega_s t_1)$

The chemical shift of spin S cosine modulates the amplitude of peak I.

1. HSQC and HMQC provide **single-bond heteronuclear shift correlations**, the correlation data are equivalent for both.
2. Historically, HSQC is favored by biological community, and presents ^{1}H-^{15}N correlations in protein molecules; HMQC is favored by chemical community, and presents ^{1}H-^{13}C correlations in small organic molecules.
3. Both HSQC and HMQC have the following 3 feathers:
   - From known proton assignments, get to know the correlated heteronucleus assignments.
   - Proton peaks disperse according to the heteronucleus shift.
   - Can identify diastereotopic geminal pairs.
4. Only difference between HSQC and HMQC is during t_1 period:
   - HSQC, only heteronulear transverse **SQ magnetization** ($-2I_zS_y$) evolves,
   - HMQC, ^{1}H-^{13}C **MQ coherence** ($-2I_xS_y$) evolves.
5. In HSQC, homonuclear ^{1}H-^{1}H couplings do not influence heteronuclear X (S_y) magnetization evolution → signals do not contain homonuclear ^{1}H-^{1}H couplings along f_1 → **improve resolution in f_1** → this is the principle advantage of HSQC over HMQC for small organic molecules.
   But HSQC use more pulses, especially 180° pulses on heteronuclears → promoting **intensity losses** from pulse miscalibration, rf inhomogeneity…

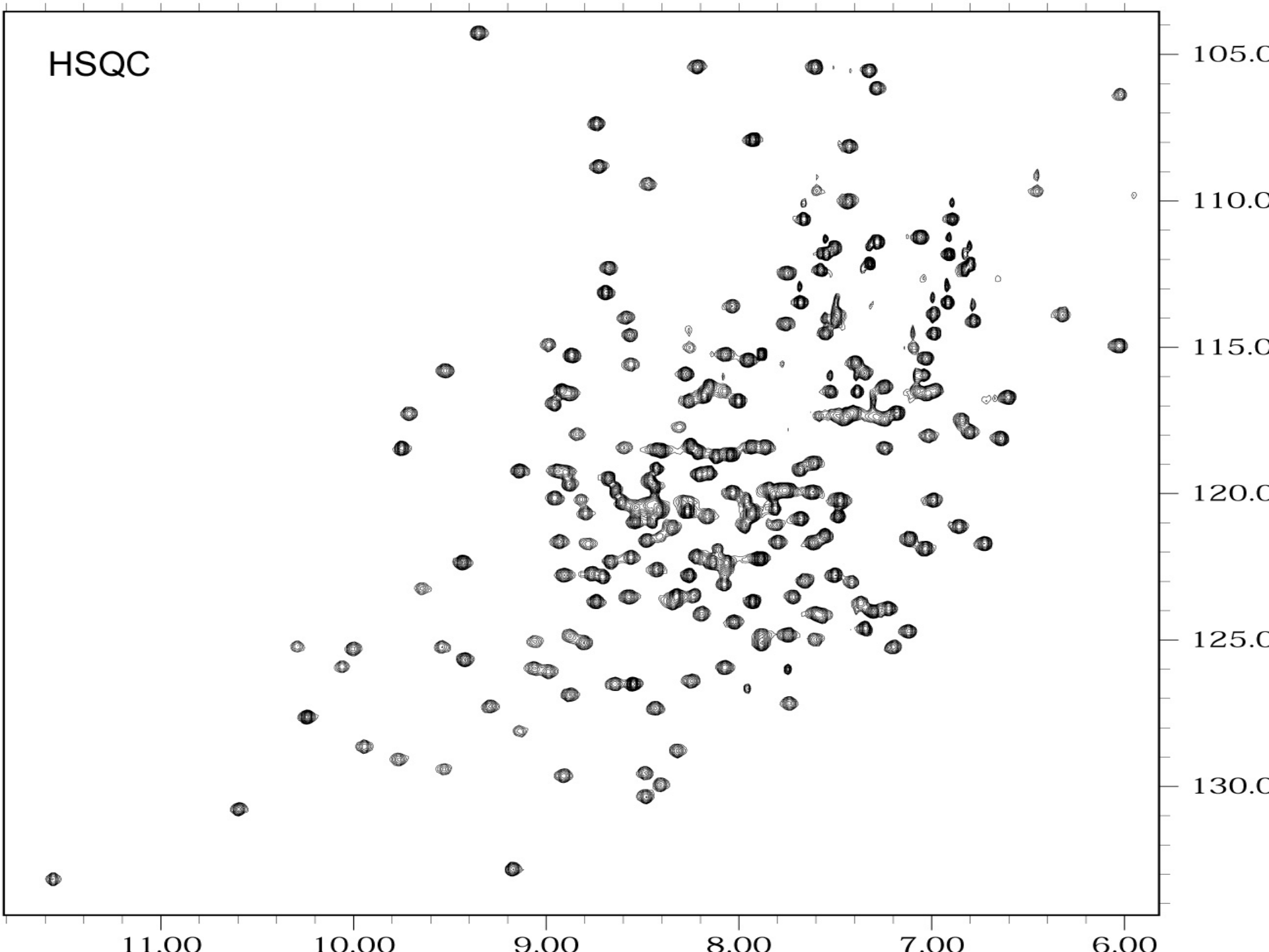
HSQC
105.0
110.0
115.0
120.0
125.0
130.0
11.00
10.00
9.00
8.00
7.00
6.00

PEP-HSQC --- "Preservation of Equivalent Pathways" developed by Rance and coworkers

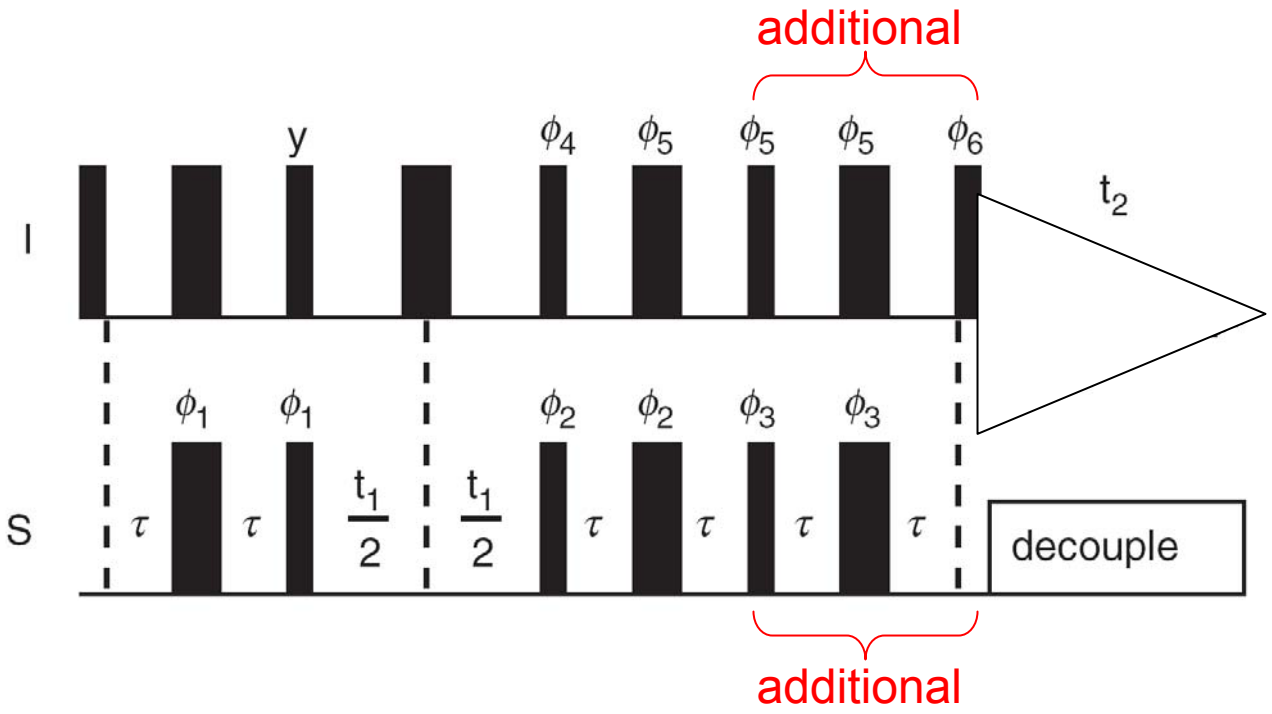

After the first INEPT, $I_z \rightarrow -2I_zS_y$, after t_1 evolution ($t_1/2$ - $\pi(I_x+K_x)$ - $t_1/2$), $-2I_zS_y \rightarrow 2I_zS_y\cos(\Omega_s t_1) - 2I_zS_x\sin(\Omega_s t_1)$; these two orthogonal terms can be preserved, and sensitivity can be improved by a factor up to $\sqrt{2}$.

When processing these kinds of 2D or 3D spectra, one should choose "Rance-Kay" as yMODE or zMODE in nmrPipe process macro.

S^3CT : spin-state-selective coherence transfer

I spin:		$180°_x$	$180°_x$
S spin:	$90°_x$ – t –	$180°_x$ – t –	$90°_y$

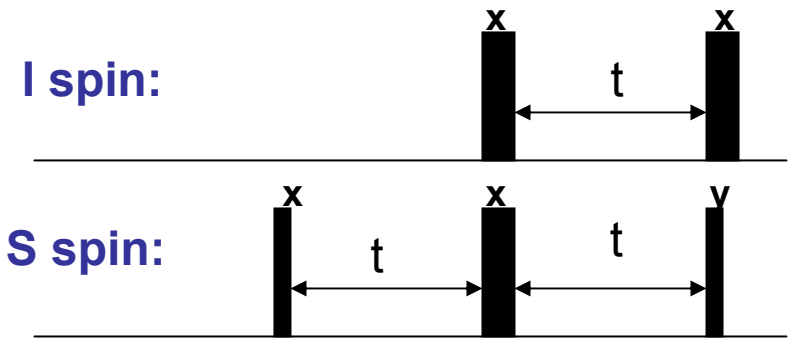

$t = 1/(4J_{IS})$

The S^3CT element can convert ZQ and DQ coherences to SQ coherence.